Coherent Light Generation from a Nd:SBN Nonlinear Laser Crystal through its Ferroelectric Phase Transition

M. O. Ramírez, D. Jaque, L. E. Bausá, and J. García Solé
Departamento de Física de Materiales, C-IV, Facultad de Ciencias, Universidad Autónoma de Madrid, Madrid 28049, Spain

A. A. Kaminskii
Institute of Crystallography, Russian Academy of Sciences, Moscow 119333, Russia
(Received 27 April 2005; published 19 December 2005)

In this Letter we have used the optical pump induced thermal loading to drive a Nd^{3+} doped $Sr_{0.47}Ba_{0.53}(NbO_3)_2$ laser crystal during laser operation through its ferroelectric phase transition. We demonstrate that lasing is possible below, at, and above phase transition. For temperatures close to T_c ($\approx 105\,^{\circ}C$) the spatial distribution of laser radiation is remarkably affected. This feature, which leads to a laser gain depression, can be explained in terms of the strong temperature dependence of the thermo-optic coefficient during phase transition. Additionally, the visible radiation generated by intracavity self-frequency doubling disappears when the phase transition is undergone, showing a bistable behavior. The results provide fundamental information on physical parameters along the phase transition and will stimulate further work in the fields of nonlinear optics, optical switching, and data storage.

DOI: 10.1103/PhysRevLett.95.267401 PACS numbers: 78.55.Hx, 42.65.Ky, 42.70.Hj, 78.45.+h

Ferroelectric crystals have been successfully used in nonlinear optical devices such as frequency doublers and mixers, optical parametric oscillators and light modulators [1–4]. When conveniently activated with optical ions they have also demonstrated laser action, which substantially increases their multifunctionality in the field of optoelectronics [5].

The case of strontium barium niobate [$Sr_xBa_{1-x}(NbO_3)_2$, hereafter SBN] crystals is of particular interest because of its relatively low phase transition temperature (ranging from $50\,^{\circ}C$ to $150\,^{\circ}C$, depending on the stoichiometry, i.e., on x). As a matter of fact, some of the most recent applications of SBN crystals, such as beam fanning reversals and polarization based adjustable memories, [6,7] are related to these relative low phase transition temperatures. On the other side, SBN crystals can be easily doped with rare earth and transition metal ions leading to novel phenomena related to the ferroelectric-to-paraelectric phase transition. For example, doping SBN with Cr^{3+} ions has shown the sensitivity of its luminescence to the phase transition, by displaying a thermally induced bistable emission related to the thermal hysteresis of the phase transition [8]. This result has supported the incorporation of other optical ions into this host, in order to investigate new bistable luminescent systems, which could be driven by light (not by an external crystal heating).

Another interesting feature of the SBN crystals is the possibility of producing laser action when doped with Nd^{3+} ions and, at the same time, of generating green coherent radiation by self-frequency doubling (SFD). This last property is related to the presence of a large density of random-size reversal ferroelectric domains in the "as-grown" crystals [9].

In this work, we have used the pump (803 nm) and intracavity stimulated emission (1060 nm) radiations to induce the crystal thermal loading needed to drive a Nd^{3+} doped $Sr_{0.47}Ba_{0.53}(NbO_3)_2$ laser crystal through a ferroelectric phase transition (at around $105\,^{\circ}C$) in the presence of laser oscillation. The effect of the ferroelectric-to-paraelectric phase transition on the near infrared laser gain (1060 nm) as well as on the SFD green radiation (530 nm) generated by SFD in random domains, has been investigated. To the best of our knowledge, this is the first time that infrared and/or visible laser action is demonstrated during the unstable situation of a phase transition. For both emerging radiations (infrared and green) light driven bistable behavior has been observed. This bistability is due to the thermal hysteresis of the phase transition and permits to envisage new optical switching devices.

The experiments have been carried out on a $Sr_{0.47}Ba_{0.52}(NbO_3)_2$ ($T_c \cong 105\,^{\circ}C$) crystal doped with 0.5 at.% of Nd^{3+} ions and grown by the Czohralski method. Laser gain experiments were performed by using a quasihemispherical cavity with a flat dichroic input mirror of high transmittance at pump wavelength and high reflectance at laser wavelength (1.06 μm). The output coupler was 10 cm radius of curvature with a transmittance of 1% for infrared laser radiation. End-pumping was performed by using a continuous-wave 100 μm fibre coupled diode laser operating at 803 nm, that is, at the maximum absorption of the ${}^4I_{9/2} \to {}^4F_{5/2}$ transition. At this pump wavelength the absorption coefficient was 3 cm^{-1}. The beam of this diode laser was collimated to give a minimum pump beam radius at the laser crystal of 90 μm. Cavity length was set to 9.5 cm, which allows for a very stable laser operation and leads to a laser beam waist of 100 μm. A $4 \times 4 \times 7$ mm^3 Nd^{3+}:SBN crystal was placed as close as possible to the input mirror. Continuous-wave laser action was achieved along its longest dimension, perpendicularly to the c axis of the crystal.

Figure 1(a) shows the laser power emitted by the crystal at 1.06 μm ($^4F_{3/2} \rightarrow {}^4I_{11/2}$ transition of Nd^{3+} ions) as a function of the absorbed pump power. Data obtained for increasing and decreasing absorbed pump power are included. The absorbed pump power was varied at a sufficiently slow rate so that both infrared laser power and crystal temperature were well stabilized all along the experiment. From Fig. 1(a), an anomalous behavior is observed for absorbed pump powers around 0.8 W (a clear depression in the output laser power takes place). In order to gain understanding on this phenomenon, we have estimated the maximum local steady-state temperature inside the Nd^{3+}:SBN crystal, T_{st}^{max}, which occurs on the cavity axis at the input crystal face. For this purpose, we have considered, in a first order approximation and according to previous models, the solution of the isotropic heat diffusion equation for a continuous wave pumped cylindrically symmetric solid-state laser [10]. This, which can be applied to the case of SBN crystals because of its almost isotropic thermal conductivity, [11] leads to

$$T_{st}^{max} = T_o + \frac{\eta_h P_{abs} \alpha_{abs}}{4\pi K_c}\left[\mathrm{Ln}\left(\frac{r_0^2}{w_p^2}\right) + 1\right] \quad (1)$$

where P_{abs} is the absorbed pump power, T_0 the temperature at the edge of the crystal on the input face, $\alpha_{abs} = 3\ \mathrm{cm}^{-1}$ the absorption coefficient at pump wavelength (803 nm), $K_{SBN} = 0.016\ \mathrm{W\,cm^{-1}\,K^{-1}}$ the room temperature thermal conductivity of SBN (corresponding to a specific heat of $0.47\ \mathrm{JK^{-1}\,g^{-1}}$) [11], $r_0 = 2$ mm the equivalent sample radius, and w_p the pump beam radius. In expression (1) η_h is the fraction of absorbed pump power which results in crystal heating. Under lasing conditions we have obtained $\eta_h = 0.23$ by considering the deexcitation from the $^4F_{5/2}$ pumping state to the $^4F_{3/2}$ metastable state and the deexcitation from the laser terminal level ($^4I_{11/2}$) to the ground state ($^4I_{9/2}$) as the relevant nonradiative channels of Nd^{3+} ions. Thus, from expression (1) we have been able to establish the steady-state maximum local temperature at the lasing volume for each absorbed pump power by using, for each case, the measured value of T_0. The results appear on the top axis of Fig. 1(a). It can be observed that in our case the light induced heating can generate local temperatures well above the transition temperature, switching the crystal from the ferroelectric to the paraelectric phase during laser operation.

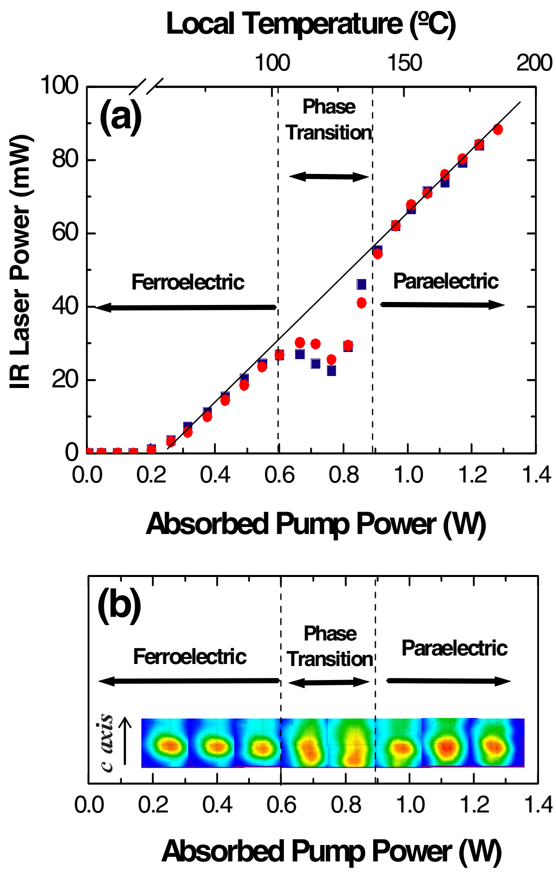

FIG. 1 (color online). (a) Infrared laser power as a function of absorbed pump power. The calculated maximum local temperature for each absorbed pump power is indicated in the top axis. Circles (red online) and squares (blue online) correspond to increasing and decreasing pump powers, respectively. (b) Spatial distribution of infrared laser beam for different absorbed pump powers.

As can be observed in Fig. 1(a), up to 0.6 W of absorbed pump power the laser crystal is in the ferroelectric phase (local temperatures are lower than 100 °C), showing the ordinary performance of a solid-state laser; i.e., a linear dependence for pump powers above threshold (0.25 W in our case). For absorbed pump powers between 0.6 and 0.9 W, the laser power deviates from the ordinary linear behavior, showing a depression in the output power with a minimum value at around 0.75 W (corresponding to a maximum local temperature of about 120 °C). For pump powers above 0.9 W (local temperatures well above phase transition), the Nd^{3+}:SBN crystal has been driven to the paraelectric phase and the laser curve recovers the linear behavior with exactly the same slope efficiency as that obtained in the starting ferroelectric phase.

The nonlinearity in the 0.6–0.9 W pump power range occurs for maximum local temperatures just above T_c indicating that this anomalous behavior is related to the phase transition. It should be noted that the behavior of SBN as a relaxor ferroelectric crystal [12] is manifested, since a phase transition extending over a finite range of temperatures (pump powers) is observed. Furthermore, as stated in previous works, the crystal temperature distribution inside longitudinally pumped solid-state lasers is far from being homogeneous [10]. In our particular case, we have estimated temperature differences between input and output faces of the order of 30 °C for an absorbed pump power of 0.8 W. Therefore, although the maximum local temperature could be above T_c, some laser active volume of the crystal could be still in the ferroelectric phase. This fact also explains why the local temperature corresponding to the deep in the laser power (120 °C) is slightly higher than T_C (105 °C). Finally, from a detailed inspection of Fig. 1(a) a hysteresis in the infrared output power is observed, this being clearly related to the thermal hysteresis characteristic of the ferroelectric-to-paraelectric phase transition in SBN crystals.

Two main reasons can account for the laser gain depression observed in Fig. 1(a). First, possible changes in the spectroscopic properties of the Nd^{3+} active ions could take place during phase transition. Secondly, changes in the spatial overlap between the pump and laser beams are induced by the phase transition, which leads to a reduction in the output power [13].

It is well-known that in the SBN crystals the ferroelectric-to-paraelectric phase transition is accompanied by some changes in the local environment around the constituting cations (Ba^{2+}, Sr^{+}, and Nb^{5+}) [14,15]. This could lead to variations in the local environment of the Nd^{3+} ions modifying their corresponding spectroscopic properties, as it was recently shown for the Cr^{3+} ion luminescence in SBN [8]. We have carefully investigated the spectroscopic properties of Nd^{3+} ions in SBN in the 25 to 200 °C range. In contrast to the Cr^{3+} case, we have found that the relevant spectroscopic parameters in laser dynamics, such as fluorescence lifetime ($\tau_F = 235 \pm 10\ \mu$s), emission cross section ($\sigma_{\rm em} = 0.2 \times 10^{-19}$ cm^2), and the fluorescence band shape of the ${}^4F_{3/2} \rightarrow {}^4I_{11/2}$ transition, are not temperature dependent in the 25–200 °C range. Thus, it is possible to conclude that the ferroelectric-to-paraelectric transition has no relevant influence in the spectroscopic parameters of Nd^{3+} ions in SBN. This is in accordance with the fact that Nd^{3+} ions in SBN crystals occupy the so called A_2 site (substituting for Sr^{2+} or Ba^{2+} cations) which are only slightly affected by the phase transition [14,15]. This fact also explains that the same laser performance (in terms of laser slope efficiency) is obtained in both the ferroelectric and the paraelectric phase.

Therefore, we expect that the laser gain depression taking place around phase transition is mainly caused by changes in the spatial overlap between the pump and laser beams. In order to confirm this fact, we have recorded the spatial distribution of the infrared output beam for each absorbed pump power. Some results are shown in Fig. 1(b) as relevant examples. For temperatures below and above phase transition the infrared output beam is Gaussian-like. For temperatures close to the phase transition, where laser gain depression occurs, a strong deformation along the ferroelectric c axis is clearly observed, according to the fact that the physical changes associated to the ferroelectric-to-paraelectric phase transition mainly occurs along this direction. Indeed, as for other ferroelectric crystals, the thermo-optic coefficient of SBN (dn/dT, where n is the refractive index and T is the temperature) displays a sharp temperature dependence near T_c [16,17]. Consequently, important thermally induced focusing and defocusing effects can occur during phase transition, leading to a strong deformation in the traveling laser beams. In the case of our Nd^{3+}:SBN laser, this deformation causes a decrease in the spatial overlap between pump and laser beams and, therefore, a decrease in the laser slope efficiency.

As previously mentioned, coherent SFD green light is also generated from our Nd^{3+}:SBN laser by means of second-harmonic generation in the randomly sized reversal ferroelectric domain structure inside the SBN crystal [9]. The dependence of the green intensity during laser action as a function of the absorbed pump power is shown in Fig. 2(a). Data obtained for increasing and decreasing absorbed power are included. In Fig. 2(b) some lateral pictures of our Nd^{3+}:SBN crystal reveal the evolution of the green light with the pump power.

To explain these results we have to take into account that the intensity of the SFD radiation depends, in a first order approximation, quadratically on the intensity of the funda-

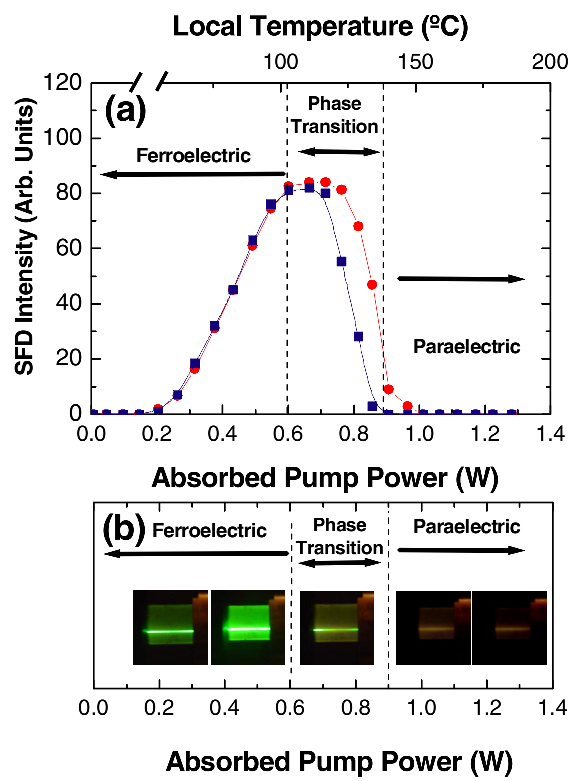

FIG. 2 (color online). (a) Self-frequency doubled intensity as a function of absorbed pump power; Circles (red online) and squares (blue online) correspond to increasing and decreasing pump powers, respectively. (b) Lateral pictures of the Nd:SBN crystal showing the diffuse green radiation generated for different absorbed pump powers.

mental radiation:

$$I_{\rm SFD} = I_{\rm IR}^2 \eta_c \tag{2}$$

where $I_{\rm SFD}$ is the SFD intensity, $I_{\rm IR}$ is the intensity of the fundamental wave, and η_c is the nonlinear infrared-to-visible conversion efficiency. The temperature dependence of the nonlinear conversion efficiency in several nonlinear ferroelectric crystals (including Nd^{3+}:SBN), has been studied in the past. In general, it is almost temperature independent in the ferroelectric phase then vanishing in the paraelectric phase [18–21]. Consequently, in the ferroelectric phase SFD intensity is expected to increase with pump power due to the linear behavior of the fundamental laser intensity [see Fig. 1(a)]. During phase transition, the power dependence of SFD intensity is governed by the drastic decrease in the nonlinear conversion efficiency. Finally, in the paraelectric phase, nonlinear conversion efficiency tends to zero and no SFD radiation is obtained.

An additional relevant feature is observed in Fig. 2(a); in the unstable region, where the phase transition takes place (0.6–0.9 W of absorbed pump power), a bistability in the SFD intensity occurs (two values of the SFD intensity exist for a given input power). The SFD intensity is higher on increasing the pump power than on decreasing it. This can be explained in terms of the characteristic thermal hysteresis associated to the first order ferroelectric transition of SBN, which presents two activation temperatures [22]. Since the nonlinear conversion efficiency is strongly dependent on the particular ferroelectric state, a thermal hysteresis is expected in the η_c conversion efficiency. Thus, we state that this thermal hysteresis is the origin of the pump-power–light driven bistabilities observed in both the SFD coherent green radiation (530 nm) and the infrared laser light (1.06 μm) generated by our diode pumped Nd:SBN laser.

In summary, we have demonstrated for the first time that stable laser action can be obtained while a ferroelectric-to-paraelectric phase transition is taking place in a solid-state laser. In our work we have used a Nd^{3+} doped SBN crystal. We have concluded that while phase transition is taking place, the anomalies caused in the thermo-optic coefficient lead to strong laser beam deformations causing a depression in the infrared laser gain. Since SBN is an efficient nonlinear crystal, simultaneous self-frequency doubling (green) light was also generated. This visible radiation has been also found to be quite sensitive to the ferroelectric-to-paraelectric phase transition, so that it vanishes when this transition takes place. On the other hand, the location of a Nd^{3+}:SBN crystal in a laser cavity produces bistable radiation at two wavelengths, 1.06 μm and 530 nm, which can be driven by the light input power. The results set the basis for new multifunction bistable optical devices.

This work has been supported by the Comunidad Autónoma de Madrid (Projects No. 07N/0020/2002 and No. GR/MAT/0110/2004), by Spanish Ministerio de Educación y Ciencia (MAT2004-03347) and by the International Association for the promotion of cooperation with scientists from the New Independent States of the former Soviet Union (INTAS), under Project No. 173. One of us (A. A. K.) acknowledges partial support from the Russian Foundation for Basic Research. The authors note also that investigation was considerably enhanced due to collaboration with the "Joint Open Laboratory for Laser Crystals and Precise Laser Systems." We thank Professor M. Bettinelli for helpful discussions.

[1] M. M. Fejer *et al.*, IEEE J. Quantum Electron. **28**, 2631 (1992).
[2] S. N. Zhu, Y. Y. Zhu, and N. B. Ming, Science **278**, 843 (1997).
[3] R. L. Byer, IEEE J. Sel. Top. Quantum Electron. **6**, 911 (2000).
[4] E. L. Wooten *et al.*, IEEE J. Sel. Top. Quantum Electron. **6**, 69 (2000).
[5] C. Becker, IEEE J. Sel. Top. Quantum Electron. **6**, 101 (2000).
[6] M. Goulkov *et al.*, J. Appl. Phys. **94**, 4763 (2003).
[7] T. Granzow *et al.*, Phys. Rev. Lett. **89**, 127601 (2002).
[8] M. O. Ramírez *et al.*, Appl. Phys. Lett. **84**, 2787 (2004).
[9] J. J. Romero *et al.*, Appl. Phys. Lett. **78**, 1961 (2001).
[10] S. Chenais *et al.*, IEEE J. Quantum Electron. **40**, 1217 (2004).
[11] C. L. Choy *et al.*, J. Appl. Phys. **71**, 170 (1992).
[12] T. R. Volk *et al.*, Phys. Solid State **42**, 2129 (2000).
[13] W. P. Risk, J. Opt. Soc. Am. B **5**, 1412 (1988).
[14] P. B. Jamieson, S. C. Abrahams, and J. L. Berstein, J. Chem. Phys. **48**, 5048 (1968).
[15] P. B. Jamieson and S. C. Abrahams, Acta Crystallogr. Sect. B **24**, 984 (1968).
[16] R. A. O'Sullivan, K. W. McGregror, and J. F. Scott, J. Phys. Condens. Matter **13**, R195 (2001).
[17] K. Sambasiva and K. H. Yoon, J. Mater. Sci. **38**, 391 (2003).
[18] R. C. Miller and A. Savage, Appl. Phys. Lett. **9**, 169 (1966).
[19] J. P. van der Ziel and N. Bloembergen, Phys. Rev. **135**, A1662 (1964).
[20] M. Zgonik, M. Copic, and H. Arend, J. Phys. C **20**, L565 (1987).
[21] J. J. Romero *et al.*, J. Appl. Phys. **93**, 3111 (2003).
[22] F. Sanchez *et al.*, Ferroelectr., Lett. Sect. **31**, 35 (2004).